Indian Journal of Pure & Applied Physics
Vol. 63, January 2025, pp. 40-50
DOI: 10.56042/ijpap.v63i1.12813

Coulomb Nuclear Interference in ^{31}Cl Breakup Reaction

Surender & Ravinder Kumar*

Department of Physics, Deenbandhu Chhotu Ram University of Science &Technology, Murthal 131 039, Sonipat, Haryana, India

Received 28 July 2024; accepted 17 December 2024

The effect of Coulomb nuclear interference on the magnitude of core fragment longitudinal momentum distribution (LMD) width and single proton breakup cross-section has been examined quantitatively for ^{31}Cl nucleus breakup reaction. The analysis is performed for ^{12}C, ^{58}Ni, and ^{208}Pb targets in a range of intermediate incident energies (40-100 AMeV), using a semiclassical method that treats the full Coulomb and nuclear interaction to all orders, including full multipole expansion of the Coulomb potential. We examined, in detail, the interference between Coulomb and nuclear diffraction reaction mechanisms and also between core-target and proton-target Coulomb potentials and quantitatively analyzed its effect on the breakup observables. The sensitivity of interference on the target size and incident energy is also examined. Our calculations show that due to the interference effect in light and heavy target cases, the absolute magnitude of a single proton breakup cross-section varies from 1% to 7%, while for medium target, it varies around 20%; on the other hand, the Full Width Half Maxima (FWHM) width of longitudinal momentum distribution varies approximately from 1% to 4% for all the target nuclei. Therefore, we believe that our work presented a bit deeper insight into the role of Coulomb nuclear interferences in ^{31}Cl breakup reaction, which is helpful for a better understanding of experimental data and planning future breakup reaction experiments.

Keywords: Coulomb nuclear interference; Proton halo breakup; LMD

1 Introduction

The study of exotic nuclei attracted a lot of attention in the last three decades because of their novel nuclear structural features and key role in astrophysical nuclear reactions[1-7]. These exotic nuclei are very loosely bound systems having core plus valence nucleon(s) nuclear structure. The small binding energy, long tail in density distribution, large matter radii, large reaction cross-section, narrow longitudinal momentum distribution of core fragment and large single nucleon breakup cross-section have appeared as the basic signature of having halo nuclear structures among these exotic isotopes[8]. In nucleosynthesis reactions, the heavy elements are synthesized through *the r*-process and *s*-process, which take place via various chain reactions of these exotic nuclei[6,9,10]. The structural properties of these exotic nuclei, therefore, act as an important input for theoretical studies of stellar reactions[10]. The study of exotic nuclei through knockout reactions has been frequently used for revealing the structural information of these nuclei[11-14], where the measurement of single nucleon breakup cross section and width of the longitudinal momentum distribution of core fragment mainly analyzed[11,15-17].

In breakup reactions, when the exotic nucleus is projected onto the target nucleus with high incident energy, the projectile nucleus breaks up into core and valence nucleon fragments due to Coulomb and nuclear interactions with the target nucleus. The dominancy of interacting potential causing the breakup mainly depends on the size of the target nucleus (atomic number of the target nucleus), i.e., in high atomic number target cases, the long-range Coulomb interaction dominates and causes the breakup, while in small atomic number target cases, nuclear interaction dominates over the other, also at low impact parameters the nuclear interaction dominates for all the targets. So, near the peripheral region (impact parameter is near to the sum of radii of projectile and target nuclei), it is very difficult to classify clearly the dominancy of Coulomb or nuclear interaction that causes the breakup of exotic nuclei. Especially for proton halo nuclei, the Coulomb dissociation reactions in the laboratory have been used indirectly to get information on radiative capture reactions because it has been shown that the Coulomb breakup cross section is proportional to the radiative capture cross-section, and hence frequently used to study stellar nucleosynthesis reactions[5-7,18-20]. So, a large number of experiments were carried out using the Coulomb dissociation mechanism[6,20,21], and mainly, single proton

*Corresponding author:
(E-mail: drravinderkumar.phy@dcrustm.org)

breakup cross-section and core fragment longitudinal momentum distribution (LMD) were measured. But in breakup reactions, these observables appeared due to the combined contribution of Coulomb and nuclear interactions, and so it is quite difficult to separate the observable magnitude corresponding to the pure Coulomb dissociation mechanism by simply subtracting the nuclear contribution from the total magnitude of the observable.

So, in this situation, a couple of questions arise: (i) Whether Coulomb and nuclear diffraction interactions interfere with each other? If yes, then what is the nature of interference, i.e. destructive or constructive? (ii) Quantitatively, how much these interferences affect the magnitude of breakup observables i.e. can vary the absolute magnitude of breakup cross-section, core fragment longitudinal momentum distribution width and other observables? (iii) How the magnitude of Coulomb nuclear diffraction interference varies with incident energy and atomic number of the target nucleus? and (iv) How does pure Coulomb interaction take place in proton halo breakup reactions? Where core-target and proton-target Coulomb interactions do exist and interfere with each other. So, to answer these questions and to extract reliable spectroscopic information from the experimental data, a good understanding of the Coulomb breakup mechanism is highly required.

A few numbers of theoretical articles using a fully quantum mechanical approach to a semi-classical approach reported their qualitative study in this direction and tried to answer the above questions[23-30]. In earlier theoretical studies for ^{8}B and ^{17}F proton halo nuclei, it has been found that Coulomb nuclear diffraction interference can have a constructive or destructive nature, which can significantly affect the magnitude of observables, and it depends upon the participating nuclei in the reaction, target size and incident energy[28,29]. A similar kind of study, ref[23,30], reported the effect of interference on angular distribution and showed that the effect is most pronounced in medium-mass targets at all beam energies.

So inspired by the significant role played by this Coulomb nuclear diffraction interference on the magnitudes of breakup observables, in the present study, we quantitatively analyzed the presence of Coulomb nuclear diffraction interference in single proton removal from ^{31}Cl reaction. We perform this investigation for ^{12}C, ^{58}Ni, and ^{208}Pb target cases in the 40-100 AMeV incident energy range, treating the Coulomb and nuclear interaction to all orders, including full multipole expansion of the Coulomb potential[23,24,26-30]. This work is carried out in the light of previous work[26-30]. In present work, our main goals are to examine quantitatively (i) the effect of Coulomb nuclear diffraction interference on the breakup observables i.e., width of core fragment longitudinal momentum distribution and single proton breakup cross-section, and its sensitivity towards target size and incident beam energy (ii) The interference among proton-target (direct) and core-target (recoil) Coulomb interactions and its affect on the magnitude of pure Coulomb breakup observables.

The ^{31}Cl nucleus is chosen here because it is a proton halo candidate and is still under investigation experimentally as well as theoretically[9,31-37]. ^{31}Cl has very small valence proton separation energy (S_p = 0.294 MeV), and as appeared from the nonlinear relativistic mean field (RMF) and relativistic density-dependent Hartree (RDDH) calculations, ^{31}C nucleus has long tail proton density distribution which reflects the large rms radii but another study at high incident energy has shown no enhancement in interaction cross-section[34], a similar study reported the possibility of new proton magic number at Z=16 with the isospin T3$\leq$ -1/2[38], which is expected to appear due to lowering of $2s_{1/2}$ orbital in ^{31}Cl nucleus that cause $1d_{3/2}$ orbital proton halo structure. Further, very recently, Y Fu *et al.*[31] experimentally measured the longitudinal momentum distribution of core fragments after single proton removal from the ^{31}Cl nucleus using a carbon target at 44AMeV incident beam energy and indicated a dominant *d*-wave component in ^{31}Cl. Also, other studies reported different spin parties (J^{π}=3/2$^-$, 1/2$^+$ or 5/2$^+$or 7/2$^+$) for ^{31}Cl nucleus, which correspond to excitation energies, i.e. 782 keV and 1793 keV, which raise the possibility of excited state halo structure in ^{31}Cl nucleus[32]. So, clear static information is missing for defining its nuclear structure that justifies its experimental observables.

Another important reason to study the ^{31}Cl nucleus is its important role in astrophysical nuclear reactions, which has attracted a lot of attention in the past few years[32,33,35-40]. In this light, recently, C. Langer *et al.*[32] investigated the thermonuclear reaction ^{30}S(p,γ)^{31}Cl via Coulomb breakup of the ^{31}Cl nucleus. They used the Coulomb breakup mechanism in inverse kinematics as a tool to investigate the capture reaction rate under typical I-x-ray burst conditions[37]. This reaction is a bottleneck during rapid proton-capture nucleosynthesis (*rp* process), where the reaction rate depends predominantly on the nuclear structure of ^{31}Cl and ONe novae study shown that the ground state

of ^{31}Cl gives the dominant reaction rate for proton-capture reaction[32]. So, keeping in view the importance of the Coulomb breakup mechanism in ^{31}Cl nuclear structural study and its role in stellar reactions, in the present study, we examined interference between Coulomb and nuclear diffraction breakup mechanisms and quantitatively analyzed its effect on the absolute magnitude of breakup observables, i.e. the width of core fragment longitudinal momentum distribution (LMD) and single proton breakup cross-section, so that we can clearly interpret the experimental data of ^{31}Cl breakup reaction and revel the clean structural information. The theoretical formalism used for this investigation is discussed in section 2, the calculated results are presented in section 3, and important conclusions are summarized in section 4.

2. Theoretical Formalism

The calculations are performed using the theoretical formalism discussed in detail in ref.[23,25-29], where projectile nucleus is assumed to have core plus valence proton nuclear structure and the Coulomb potential between projectile and target nucleus, causing the breakup, can act both on the core and on the valence proton, and is defined as

$$V(\vec{r},\vec{R}) = \frac{V_c}{|\vec{R}-\beta_1\vec{r}|} + \frac{V_v}{|\vec{R}+\beta_2\vec{r}|} - \frac{V_0}{|\vec{R}|} \quad ...(1)$$

where, $V_c = Z_c Z_t e^2$, $V_v = Z_v Z_t e^2$, and $V_0 = (Z_c + Z_v)\, Z_t e^2$ are the core-target, valence proton-target and whole projectile-target Coulomb potentials and Z_c, Z_v and Z_t are the atomic number of core, valence proton and target nucleus respectively. β_1 and β_2 are the mass ratios of proton and core to the projectile mass. Also, $\vec{r}$ and $\vec{R}$ are the core-proton and target-projectile position vectors respectively, as shown in the coordinate system in ref.[28,30].

The perturbed Coulomb phase for the entire projectile (comprise with core and valence proton) is given by[26-28,30]

$$\chi^p = \frac{2}{\hbar v}\Big(V_c e^{i\beta_1\omega z/v} K_0(\omega b_c/v) + V_v e^{-i\beta_2\omega z/v} K_0(\omega b_v/v) - V0K0\omega R\perp/v \quad ...(2)$$

here, $\omega = (\varepsilon_f - \varepsilon_0)/\hbar$, with ε_0 and ε_f are the valence proton separation energy and the final proton-core continuum energy, K_0 is the Modified bessel function, b_v and b_c are the individual impact parameter of valence proton and core with the target, respectively and v is the velocity of the projectile in z-direction.

The total projectile Coulomb potential (V_0) with the target can be expressed as the simple sum of the core-target (V_c) and valence proton-target (V_v) Coulomb potentials, i.e., $V_0 = V_c + V_v$ and thus, the entire projectile's perturbed Coulomb phase (Eq. 2), can be written as

$\chi^p = \chi(\beta_1, V_c, b_c) + \chi(-\beta_2, V_v, b_v)$, where,

$$\chi(\beta_1, V_{c,} b_{c,}) = \frac{2V_c}{\hbar v}\Big(e^{i\beta_1\omega z/v} K_0(\omega b_c/v) - K_0(\omega R_\perp/v)\Big) ...(3)$$

$$\chi(-\beta_2, V_{v,} b_v) = \frac{2V_v}{\hbar v}\Big(e^{-i\beta_2\omega z/v} K_0(\omega b_v/v) - K_0(\omega R_\perp/v)\Big) \quad ...(4)$$

These phases correspond to the core-target and the valence proton-target Coulomb phases, respectively.

The Coulomb breakup mechanism has always been suggested to treat with all orders including all multipolarities, specially in proton halo breakup reactions, its significance have been emphasized in a number of theoretical studies[29,31,32,36]. Therefore, in this work we also treated both i.e. core-target (referred to as "Recoil interaction") and valence proton-target (referred to as "Direct interaction"), the Coulomb interaction to all orders including full multipole expansion of the Coulomb potential[23,25], in which the core-target (Recoil) and valence proton-target(Direct) Coulomb amplitudes can be expressed as

$$g^{rec}(b_c) = \int d\vec{r} e^{-i\vec{k}\cdot\vec{r}} \phi_i(\vec{r}) \Bigg(e^{i\frac{2V_c}{\hbar v}\log\frac{b_c}{R_\perp}} - 1 - i2Vc\hbar v\log bcR\perp + i\chi\beta 1,Vc,bc \quad ...(5)$$

$$g^{dir}(b_v) = \int d\vec{r} e^{-i\vec{k}\cdot\vec{r}} \phi_i(\vec{r}) \Bigg(e^{i\frac{2V_v}{\hbar v}log\frac{b_v}{R_\perp}} - 1 - i2Vv\hbar vlogbvR\perp + i\chi-\beta 2,Vv,bv \quad ...(6)$$

while the pure nuclear diffraction dissociation is treated with Glaubereikonal approximation, and its amplitude is expressed as[29]

$$g^{diff}(b_v) = \int d\vec{r} e^{-i\vec{k}\cdot\vec{r}} \phi_i(\vec{r}) |S_{vt}(b_v) - 1| \quad ...(7)$$

And so the core fragment differential momentum distribution including Coulomb and nuclear diffraction dissociation mechanism amplitudes is given by

$$\frac{d\sigma}{d\vec{k}} = \frac{1}{8\pi^3}\int d\overrightarrow{b_c}|S_{ct}(b_c)|^2|g^{rec} + g^{dir} + g^{diff}|^2 \quad ...(8)$$

and the core longitudinal momentum distribution (LMD) is obtained by integrating the differential momentum distribution i.e. Eq.(8) over the transverse momentum components $k_\perp(k_x, k_y)$ i.e.

$$\frac{d\sigma}{dk_Z} = \int \frac{d\sigma}{d\vec{k}}\, dk_\perp\left(k_x, k_y\right) \quad ...(9)$$

and it gives

$$\frac{d\sigma}{dk_z} = \frac{1}{2\pi}\int d\overrightarrow{b_c}|S_{ct}(b_c)|^2|g^{rec} + g^{dir} + g^{diff}|^2 \quad ...(10)$$

and then single proton breakup cross section is obtained by integrating the longitudinal momentum distribution i.e. Eq. (10) over the longitudinal momentum i.e. (k_z).

Here, $S_{\rm ct}(b_c)$ and $S_{\rm vt}(b_v)$ are the core-target and valence proton-target nuclear interactions i.e. *S*-matrices or profile functions, calculated using the Hartree-Fock nuclear density forms of core and target nuclei[41,42], using MOMDIS code[43]. The bound state projectile wave function ($\phi_i(\vec{r})$), in core plus valence proton configuration $[0^+ \otimes 1d_{3/2}]$, is calculated by numerically solving the Schrodinger wave equation with Woods-Saxon(WS) nuclear potential (V_0=45.36 MeV)[43]. The depth of the WS nuclear potential is adjusted to reproduce the separation energy (S_p= 0.264 MeV) of the valence proton, while the range (r_0), diffuseness (a_0) and the spin orbit potential depth (V_{ls}) parameters are kept 1.27fm, 0.7fm and 17 MeV respectively as used in ref.[31].

3 Results and Discussion

Using the above theoretical formalism, the magnitudes of longitudinal momentum distribution (LMD) width of core fragment and single proton breakup cross-section are calculated for ^{31}Cl breakup reaction exclusively for different targets, i.e., ^{12}C, ^{58}Ni, and ^{208}Pb targets, at 40, 60, 80 and 100 AMeV incident beam energies. We calculated the absolute values of these observables separately and together due to pure Coulomb (recoil plus direct interaction) and nuclear diffraction breakup mechanism and then showed how the interference modified the simple sum of the observable values.

We assumed ^{31}Cl nucleus to be a two-body system have a core (^{30}S) plus loosely bound valence proton (S_p=0.294 MeV) nuclear structure, having $[0^+ \otimes 1d_{3/2}]$ core plus valence proton projectile configuration, as frequently reported in ref.[35]. were strict our analysis for the frequently reported projectile configuration $[0^+ \otimes 1d_{3/2}]$, the other possible projectile configurations are not considered in this work and hopefully be examine in our next paper.

The chosen observables reveal efficiently the nuclear structure of the projectile nuclei and are frequently used as a reliable tool for halo structural studies[14]. Therefore, the interference among breakup mechanisms and its effect on the absolute magnitude of observables becomes very important for the lucid interpretation of the nuclear structure. Here, we have not included the proton stripping contribution in this interference study because, in the stripping mechanism, the valence nucleon is stripped off (absorbed) by the target nucleus, and it is not detected in the coincidence measurements with the residue core fragment, so stripping mechanisms neither interfere with diffraction nor with Coulomb breakup mechanism.

3.1 Effect of Coulomb nuclear diffraction interference on the breakup observables

We calculated both the observables exclusively for nuclear diffraction and total pure Coulomb mechanism, including recoil and direct interactions (termed as "Coulomb (total)" in the text) and also inclusively for both total Coulomb and nuclear diffraction dissociation mechanisms (termed as "Coul+Diff. (cal. together)" in the text). The obtained magnitudes of single proton breakup cross-section and Full Width Half Maxima width of core fragment longitudinal momentum distribution (LMD) spectrum for ^{12}C, ^{58}Ni and ^{208}Pb targets at 40, 60, 80 and 100 AMeV incident beam energies are shown in Table 1-3 respectively. The percentage change in the observable values due to Coulomb nuclear diffraction interference is obtained by the formula:

$$\%\, change = \frac{X^{Coul+Diff} + (X^{Coul} + X^{Diff.})}{(X^{Coul} + X^{Diff.})} \times 100\% \quad ...(11)$$

where $X^{Coul+Diff}$ stand for breakup cross-section or FWHM width of LMD when Coulomb and nuclear diffraction calculated together while $(X^{coul} + X^{Diff.})$ stand for simple algebraic sum of observable exclusively calculated in Coulomb and nuclear diffraction dissociation mechanisms. For the sake of

Table 1 — Calculated single proton breakup cross-section and FWHM of longitudinal momentum distribution(LMD) of core fragment in ^{31}Cl breakup reaction with ^{12}C target at different incident beam energies exclusively for nuclear diffraction, total pure Coulomb(total)(containing direct and recoil interactions) and inclusivlely for Coulomb(total) with nuclear diffraction dissociation mechanisms. The percent change in magnitudes of observables are shown on the bottom.

Reaction Mechanisms	E_{lab} 40 AMeV		60AMeV		80AMeV		100 AMeV	
	σ (mb)	FWHM (MeV/c)	σ (mb)	FWHM (MeV/c)	σ (mb)	FWHM (MeV/c)	σ (mb)	FWHM (MeV/c)
Diff.	5.88	159.14	8.72	168.58	8.01	169.18	5.99	170.09
Coul. (total)	4.91	125.48	4.02	133.09	3.54	138.57	3.18	141.94
Coul. +Diff. (simple sum)	10.80	140.89	12.74	153.71	11.55	156.99	9.17	157.91
Coul.+Diff. (cal. together)	11.43	140.98	12.57	152.25	11.05	155.59	8.50	156.45
% Change	+5.83	+0.06	-1.33	-0.94	-4.33	-0.89	-7.30	-0.92

Table 2 — Same as Table 1, but for ^{58}Ni target

Reaction Mechanisms	E_{lab} 40 AMeV		60AMeV		80AMeV		100 AMeV	
	σ (mb)	FWHM (MeV/c)	σ (mb)	FWHM (MeV/c)	σ (mb)	FWHM (MeV/c)	σ (mb)	FWHM (MeV/c)
Diff.	8.64	153.43	11.96	160.43	11.39	160.88	9.76	158.89
Coul. (total)	104.51	122.02	75.41	124.27	62.55	127.48	54.44	130.10
Coul.+Diff. (simple sum)	113.15	124.11	87.37	128.06	73.94	131.39	64.20	133.46
Coul.+Diff. (cal. together)	133.90	129.76	105.04	132.94	87.92	135.23	75.34	136.47
% Change	+18.34	+4.55	+20.22	+3.81	+18.91	+2.92	+17.35	+2.25

Table 3 — Same as Table 1 and Table 2, but for ^{208}Pb target.

Reaction Mechanisms	E_{lab} 40 AMeV		60AMeV		80AMeV		100 AMeV	
	σ (mb)	FWHM (MeV/c)	σ (mb)	FWHM (MeV/c)	σ (mb)	FWHM (MeV/c)	σ (mb)	FWHM (MeV/c)
Diff.	12.23	151.54	17.33	159.44	16.21	158.80	13.09	155.09
Coul.(total)	1931.54	160.54	1103.97	147.80	778.67	141.73	603.25	136.56
Coul.+Diff. (simple sum)	1943.77	160.46	1121.30	148.02	794.87	142.09	616.35	138.92
Coul.+Diff. (cal. together)	1975.16	162.87	1178.60	151.51	848.87	145.65	664.70	142.49
% Change	+1.61	+1.50	+5.11	+2.36	+6.36	+2.45	+7.84	+2.50

simplicity, the spectroscopic factor for the initial state is taken unity throughout the calculations. Table 1 shows the absolute magnitudes of observables in ^{12}C(^{31}Cl,^{30}S)X reaction for 40, 60, 80, and 100 AMeV incident beam energy, where values corresponding to diffraction, total Coulomb and total Coulomb plus diffraction are shown separately. It is clear from Table 1 that at 40 AMeV beam energy, the Coul.+Diff. (cal. together) shows slightly more absolute values for both single proton breakup cross-section and FWHM of LMD width, in comparison to the simple sum of exclusively calculated magnitudes of observables for Coulomb and nuclear Diffraction (simple sum). This indicates the presence of constructive interference between Coulomb and diffraction dissociation mechanisms, which enhance the magnitude of the breakup cross section by approximately 5.8% and LMD width by 0.06%. While in 60, 80, and 100 AMeV incident energy cases, the magnitude of observables in Coul.+Diff. (cal. together) is less in comparison to the simple sum of exclusively calculated magnitudes of observables (Coulomb and nuclear diffraction (simple sum)), which indicates the presence of destructive

interference which reduces the breakup cross-section approximately by 1.3%, 4.3%, and 7.3%, respectively, and it seems increasing with rise in incident beam energy. Whereas, the FWHM of LMD width also experiences feebly destructive interference, due to which LMD width reduces by less than 1% for all the incident beam energies, which indicates that the effect of Coulomb nuclear diffraction interference on LMD width is very small and does not vary with the rise in incident energy in 60-100 AMeV range for ^{12}C target.

Similarly, Table 2 shows the results for ^{58}Ni(^{31}Cl, ^{30}S)X reaction for 40, 60, 80, and 100 AMeV incident beam energies. Here, Coul.+Diff. (cal. together) show significantly more absolute values for both single proton breakup cross-section and FWHM of LMD width for all the incident beam energy cases, in comparison to the simple sum of exclusively calculated magnitudes of observables, i.e. Coulomb and nuclear diffraction (simple sum). This indicates the presence of constructive interference in this reaction, which enhances the breakup cross-section by approximately 17%-20%, respectively, and it shows a very small dependence on incident beam energy. Whereas, the 4.5% to 2.2% enhanced LMD width also indicates the presence of constructive interference, and this percent change in LMD width decreases with rise in incident energy. This significant variation in the breakup cross-section is consistent with the results of ref[30]. Similarly, the results of ^{208}Pb(^{31}Cl, ^{30}S)X reaction at 40, 60, 80, and 100 AMeV incident beam energies are shown in Table 3, where again the Coul.+Diff. (cal. together) shows slightly more absolute values for both single proton breakup cross section and FWHM of LMD width for all the incident beam energy cases, in comparison to their simple sum of exclusively calculated magnitude, which indicate the presence of constructive interference in these reactions, which enhances the breakup cross-section approximately 1% to 7%, and this percentage change increases with incident beam energy. Similarly, the FWHM of LMD width also experiences constructive interference, which enhances the LMD width by approximately 1.5% to 2.5% and is very slightly sensitive to the rise in incident energy.

For the sake of clarity, the percentage variation in magnitude of single proton breakup cross-sections (Fig. 1(a)) and FWHM width of LMD distributions (Fig. 1(b)) with incident beam energy are shown in Fig. 1. It is quite clear from Fig. 1 that the percentage variation in magnitude of observables due to Coulomb nuclear diffraction interference is relatively small for

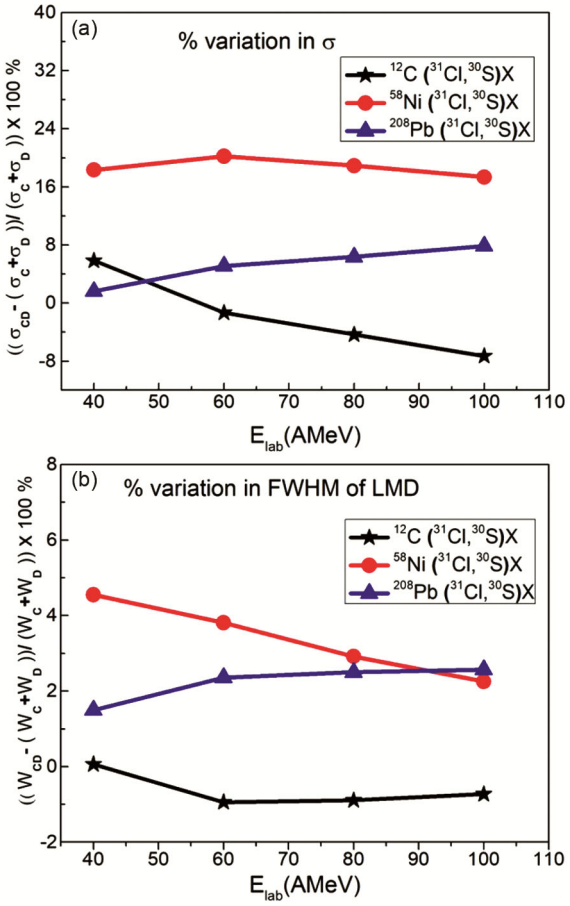

Fig. 1 — (a) Percent variation in magnitude of single proton breakup cross section with incident energy (E_{lab}) and (b) percent variation in Full Width Half Maxima(FWHM) of longitudinal momentum distribution (LMD) width with incident energy(E_{lab}).

light and heavy target nuclei, *i.e.* ^{12}C and ^{208}Pb in comparison to medium target, *i.e.* ^{58}Ni nucleus, which is qualitatively well consistent with the fact that in case of the light target, the Coulomb interaction is small, so nuclear interaction dominates and on the other hand in heavy target case Coulomb interaction dominates over the nuclear interaction, so interference among the breakup mechanisms is small due to which the variation in magnitude values is small. However, in the medium target, ^{58}Ni case, both Coulomb and nuclear interaction dominate equally in the breakup, and that is why interference between this dissociation mechanism is greater in comparison to light or heavy targets. Also, here we would like to mention that besides a qualitative understanding of this mechanism, it is very important to examine quantitatively the effect of this interference on the absolute magnitudes of breakup observables, which is quite helpful for better interpretation of experimental results for clear structural information and also planning

new experiment. To the best of our knowledge, this is the first time we have quantitatively investigated the effect of Coulomb nuclear diffraction interference on the breakup observables in ^{31}Cl breakup reaction with different choices of target and frequently used incident beam energies.

3.2 Interference between Direct and Recoil Coulomb interactions in pure Coulomb mechanism

As discussed in the introduction and in refs[26-27], the pure Coulomb breakup mechanism of proton halo nuclei is quite different to that of neutron halo breakup, where the Coulomb breakup is caused only by the repulsive Coulomb interaction between the incoming core of the projectile and target nucleus, but in proton halo case the situation is more complicated because not only the core of projectile experience the Coulomb repulsion (recoil Coulomb interaction) but also the valence proton experience the Coulomb repulsion (direct Coulomb interaction) at the same time due to target nucleus. During the time of interaction, the proton-target (direct) Coulomb potential interferes with core-target (recoil) Coulomb potential and affects the pure Coulomb breakup observable's magnitude, as reported in ref.[26-27,30]. Therefore, we have also exclusively investigated the interference between core-target Coulomb interaction (recoil interaction) and valence proton-target Coulomb interaction (direct interaction) for the chosen targets and incident beam energy range.

We calculated LMD distribution and single proton breakup cross-section for pure Coulomb breakup mechanism, exclusively for direct recoil interactions and direct plus recoil interaction together (including the interference). The obtained values of observables are shown in Table 4-6 for ^{12}C, ^{58}Ni and ^{208}Pb targets, respectively, for 40, 60, 80 and 100 AMeV incident beam energies.

It is quite clear from Table 4, that values of both the observables corresponding to direct interaction (being proportional to β_2), are always larger than the values of recoil interaction, and when pure Coulomb breakup cross-section is calculated with both recoil and direct interactions, the magnitude of breakup cross-section reduced by approximately 72% to 75% than that of their simple sum (when direct and recoil are calculated separately and algebraically added), this clearly show that proton-target (direct) Coulomb interaction introduce destructive interference, due to

Table 4 — Calculated single proton breakup cross-section and FWHM of longitudinal momentum distribution width of ^{31}Cl breakup reaction with ^{12}C target at different incident beam energies corresponding to Recoil, Direct and Recoil plus Direct (Coulomb (total)) mechanisms, the respective percent change in observable values are also on the bottom row shown.

Reaction Mechanisms	E_{lab} 40 AMeV		60AMeV		80AMeV		100 AMeV	
	σ (mb)	FWHM (MeV/c)	σ (mb)	FWHM (MeV/c)	σ (mb)	FWHM (MeV/c)	σ (mb)	FWHM (MeV/c)
Recoil	3.54	116.83	3.15	124.09	2.86	128.92	2.61	132.19
Direct	14.38	117.21	12.63	125.14	11.40	130.56	10.36	134.03
Direct+Recoil (simple sum)	17.92	117.04	15.78	127.77	14.26	130.05	13.22	132.66
Coul.(total) (cal. together)	4.91	125.48	4.02	133.09	3.54	138.57	3.18	141.94
% Change	-72.60	+7.21	-74.52	+4.16	-75.17	+6.55	-75.94	+6.98

Table 5 — Same as Table 2, but for ^{58}Ni target.

Reaction Mechanisms	E_{lab} 40 AMeV		60AMeV		80AMeV		100 AMeV	
	σ (mb)	FWHM (MeV/c)	σ (mb)	FWHM (MeV/c)	σ (mb)	FWHM (MeV/c)	σ (mb)	FWHM (MeV/c)
Recoil	57.01	109.50	50.83	115.76	46.74	120.55	43.27	123.94
Direct	227.65	108.99	198.05	115.53	180.42	120.52	106.18	124.03
Direct+ Recoil (simple sum)	284.66	109.13	248.88	115.57	227.16	120.49	209.46	123.95
Coul.(total) (cal. together)	104.51	122.02	75.41	124.27	62.55	127.48	54.44	130.10
% Change	-63.31	+11.81	-69.70	+7.57	-72.46	+5.80	-74.01	+4.96

Table 6 — Same as Table 2, but for ^{208}Pb target

Reaction Mechanisms	E_{lab}							
	40 AMeV		60AMeV		80AMeV		100 AMeV	
	σ (mb)	FWHM (MeV/c)	σ (mb)	FWHM (MeV/c)	σ (mb)	FWHM (MeV/c)	σ (mb)	FWHM (MeV/c)
Recoil	387.60	104.28	330.89	109.34	301.00	113.14	277.83	116.05
Direct	1874.19	112.99	1402.31	112.83	1205.96	114.87	1082.03	117.16
Direct+ Recoil (simple sum)	2261.80	111.07	1733.21	112.11	1506.96	114.53	1359.86	116.95
Coul.(total) (cal. together)	1931.54	160.54	1103.97	147.80	778.67	141.73	603.25	136.56
% Change	-14.60	+44.54	-36.30	+31.83	-48.33	+23.75	-55.66	+16.77

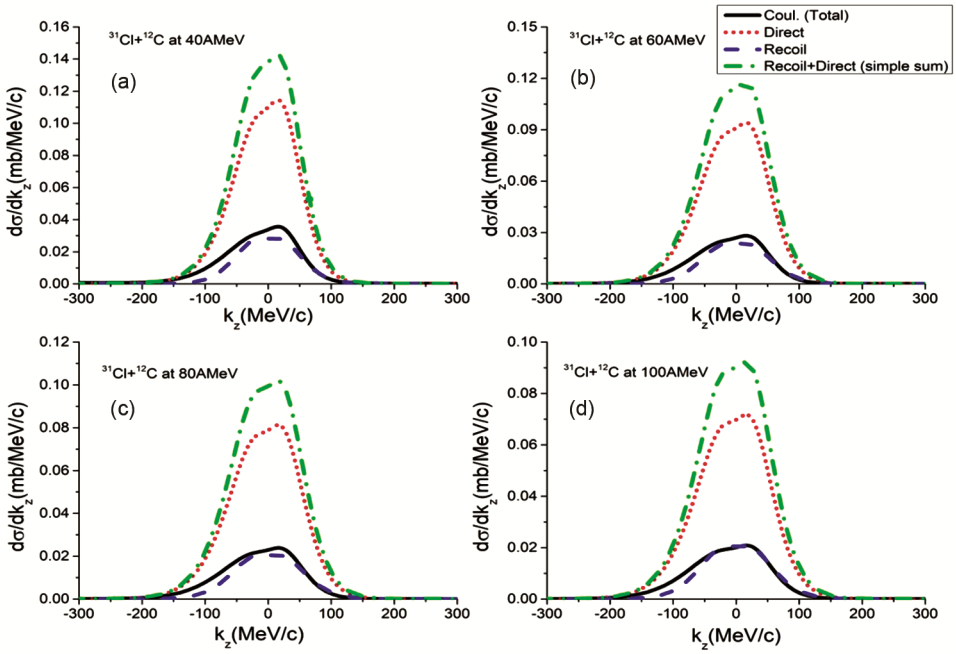

Fig. 2 — The longitudinal momentum distribution for ^{31}Cl breakup reaction with ^{12}C target at 40, 60, 80 and 100 AMeV beam energies, where the solid Black curve corresponds to Recoil plus Direct Coulomb interaction [Coul.(total)], Red dotted curve and Blue dashed curve corresponds to Direct and Recoil interaction respectively, while Green dashed-dotted curve corresponds to simple sum of separately calculated Recoil and Direct Coulomb interactions.

which size of total Coulomb LMD curve reduce and hence the magnitude of breakup cross-section significantly reduces, this trend is observed for all the considered incident beam energies. On the other hand the FWHM width of LMD distribution increases approximately 4% to 7%. A mild dependence of destructive interference on incident energy is notice in this reaction. To give a better insight of destructive interference, the plots of LMD distribution corresponding to direct, recoil and recoil plus direct Coulomb interactions for each incident energy are shown in Fig. 2. Similarly, for the ^{58}Ni target case, the interference between direct and recoil interaction is found to be of a destructive nature, which reduces the size of the LMD curve and hence reduces the single proton breakup cross section by approximately 63% to 74% and increases the LMD width by approximately 11% to 4% respectively with increase incident energy. Small dependence on incidence energy can be seen in both the observables. For clarity, the LMD curves of recoil, direct, total Coulomb (containing recoil and direct) and simple sum of recoil and direct Coulomb interaction are shown in Fig. 3 for all the incident energies. In the case of the ^{208}Pb target, again, the destructive interference is observed among direct and recoil

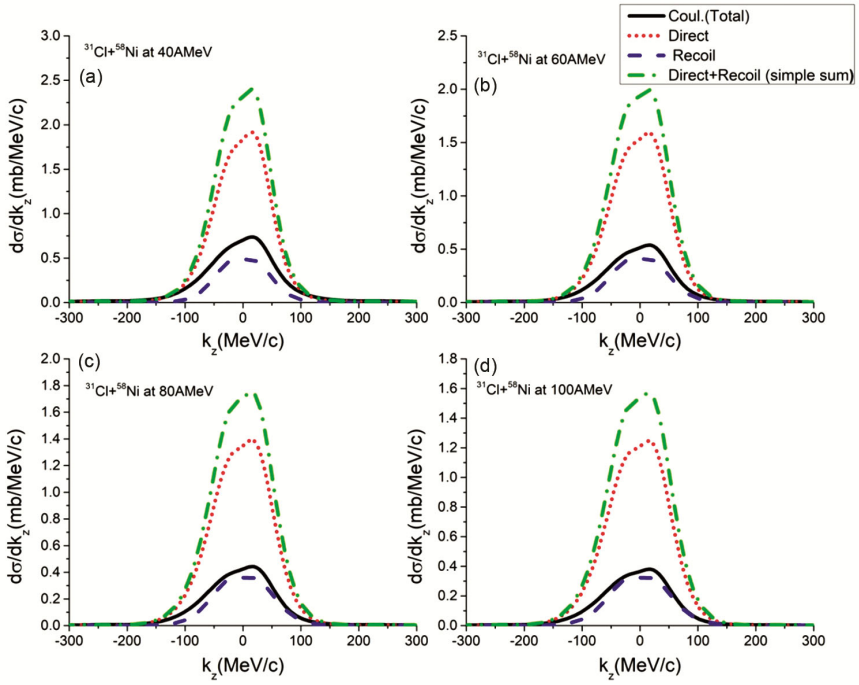

Fig. 3 — Same as Figure 2 but for ^{58}Ni target.

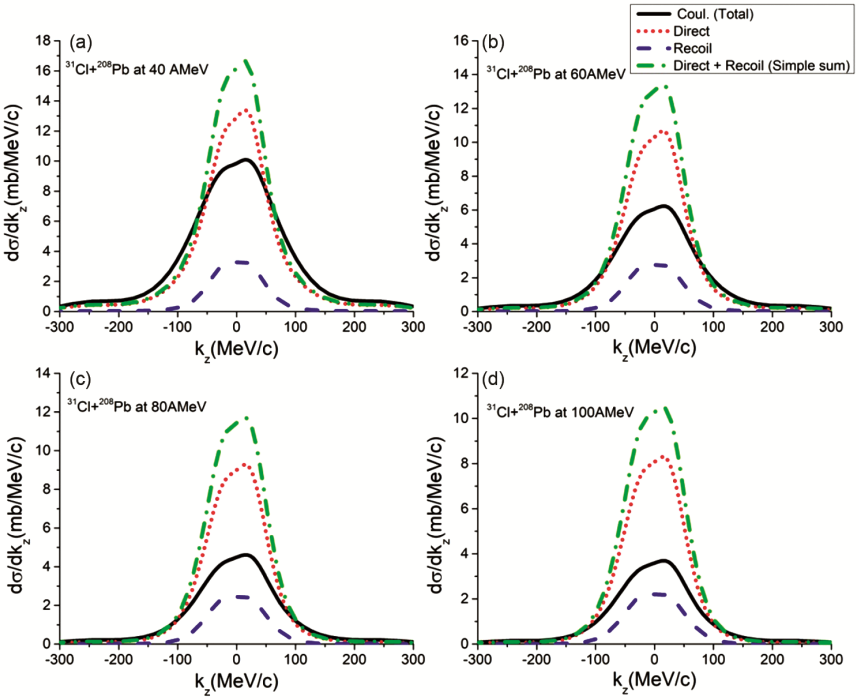

Fig. 4 — Same as Figure 3, but for ^{208}Pb target.

terms, which reduces the single proton breakup cross-section from 14% to 55%, and this percentage increases with the rise in incident energy while the LMD width varies from 44% to 16%, and this percentage decreases with rise in incident energy, the respective LMD curves are shown in Fig. 4. The obtained trend of our results is consistent with our previous work of ^{17}F and ^{8}B[28], however destructive or constructive nature of interference varies from nucleus to nucleus and sensitive to the size of target

nucleus (atomic number of target nucleus) and also on the incident energy of the projectile nucleus. The nature of interference depends on the valence proton target interaction that in fact appears through optical potential and Coulomb repulsion, and these varies with incident energy[23]. Thus, we found that role of proton-target interaction plays a critical role in the dynamics of the proton halo breakup reactions, which is more complicated than that of neutron halo breakup reactions, and such a concept will have to be handled with great care while dealing with proton halo breakup reactions.

4 Conclusion

We conducted an investigation for ^{31}Cl nucleus breakup reactions for three different targets, ^{12}C, ^{58}Ni, and ^{208}Pb nucleus, for intermediate incident energies, i.e. 40 to 100 AMeV. Our focus has been to examine the presence of interference in (i) Coulomb and nuclear diffraction dissociation mechanisms and (ii) core-target and proton-target Coulomb potentials in these breakup reactions and quantitatively estimate the effect of interference on the width of core fragment longitudinal momentum distribution and magnitude of single proton breakup cross-section. Our calculations reveal that Coulomb nuclear diffraction interference does exist in these breakup reactions and significantly affects the magnitude of both breakup observables. Depending upon the target nucleus size and incident energy, interference shows a destructive or constructive nature, which leads to reduction or enhancement in the absolute magnitude of a single proton breakup cross-section, and it may vary the magnitudes from 1 % to 7 % for ^{12}C and ^{208}Pb targets, while for ^{58}Ni target it is 17 % to 20 % for 40-100 AMeV incident energy range. On the other hand, the width of core fragment longitudinal momentum distribution (LMD) varies between 1% and 4% for all the target cases and slightly depends on the incident beam energy. Also, in the pure Coulomb breakup mechanism, we noticed that proton-target (direct) Coulomb interaction always plays a destructive role with the core-target (recoil) Coulomb interaction process, which significantly reduces the total Coulomb breakup cross-section, and due to which the size of longitudinal momentum distribution spectrum reduces, giving enhancement in the FWHM width, similar trend is observed for all the chosen target nuclei and incident beam energies. The constructive or destructive nature of interference depends on the valence proton target imaginary optical potential which tends to vary with beam energy, as studied in ref.[23,29] the proton target interaction is more complicated than that of neutron target interaction in case of proton halo breakup reactions. Thus, it is clear from these results that Coulomb nuclear diffraction interference always exists in proton knockout reactions in proton rich nuclei which behaves destructively or constructively during the reaction and ultimately affects the absolute magnitudes of breakup observables. So, Interference effects on observables are impossible to predict without an explicit calculation, particularly for nuclear astrophysics applications where Coulomb breakup is considered the inverse of proton capture reaction, the study of interference effect is quite important. Finally, this is the first time, we presented a detailed quantitative assessment of Coulomb nuclear interference in ^{31}Cl breakup reaction, which would definitely be helpful in the interpretation of its experimental data and revealing clear structural information, which is quite important for a better understanding of nucleosynthesis reactions and planning new experiments in the near future.

Competing Interests

The authors declare no competing financial interest.

Acknowledgments

We are thankful to Prof. Angela Bonaccorso, INFN, Italy, for fruitful discussion time to time.

References

1 Tanihata I, Hamagaki H, Hashimoto O, Shida Y, Yoshikawa N, Sugimoto K & Takahashi N, *Phys Rev Lett*, 55 (1985) 2676.
2 Tanihata I, Hamagaki H, Hashimoto O, Nagamiya S, Shida Y, Yoshikawa N, Yamakawa O, Sugimoto K, Kobayashi T, Greiner D E & Takahashi N, *Phys Lett B*, 160 (1985) 380.
3 Jensen A S, Riisager K & Fedorov D V, *Nucl Phys A*, 688 (2001) 563.
4 Bertulani C A & Arne G, *Phys Rep*, 485 (2010) 195.
5 Baur G, Bertulani C A & Rebel H, *Nucl Phys A*, 458 (1986) 188.
6 Iwasa N, Motobayashi T, Ando Y, Kurokawa M, Moriya S, Murakami H, Nishio T, Gen J R, Shirato S & Yanagisawa T, *J Phys Soc Jpn*, 65 (1996) 1256.
7 Schümann F, Aumann T, Banu A, Boretzky K, Elze T W, Geissel H, Grasse M, Kulessa R, Leifels Y & Leistenschneider A, *Phys Rev C*, 73 (2006) 015806.
8 Al-Khalili J, *In the Euroschool Lectures on Physics with Exotic Beams*, Berlin, Heidelberg, Springer Berlin Heidelberg, 1 (2004) 77.
9 Kankainen A, Penttilä H, Leppänen A P, Batchelder J C, Bingham C R, Jeppesen H B, Lee J K P, Loveland W, Lukyanov S & Uusitalo J, *Eur Phys J A*, 27 (2006) 67.
10 Baur G & Heinrich R, *Ann Rev Nucl Part Sci,* 46 (1996) 321.
11 Sauvan E F, Carstoiu N A, Orr J S, Winfield M F, Angélique

J C, Catford W N, et al., *Phys Rev C,* 69 (2004) 044603.
12 Chatterjee R, Banerjee P & Shyam R, *Nucl Phys A*, 675 (2000) 477.
13 Chatterjee R, *Phys Rev C*, 75 (2007) 064604.
14 Thompson I J, *Exotic Nuclei and Atomic masses* (ENAM 98), 455 (1998) 174.
15 Bertulani C A & McVoy K W, *Phys Rev C*, 46 (1992) 2638.
16 Kelley J H, Sam M A, Kryger R A, Morrissey D J, Orr N A, Sherrill B M, Thoennessen M, Winfield J S, Winger J A & Young B M, *Phys Rev Lett*, 74 (1995) 30.
17 Shubhchintak, *Phy Rev C*, 96 (2017) 024615.
18 Utsunomiya H & Typel S, *Nuclei Far Stability Astrophys*, (2001) 259.
19 Rebel H, Nucl Astrophys: *Proc Workshop Ringberg Castle Tegernsee*, (2005) 38.
20 Motobayashi T, Iwasa N, Ando Y, Kurokawa M, Moriya S, Murakami H, Nishio T, Gen J R, Shirato S & Yanagisawa T, *Phys Rev Lett*, 73 (1994) 2680.
21 Kikuchi T, Motobayashi T, Iwasa N, Ando Y, Kurokawa M, Moriya S, Murakami H, Nishio T, Gen J R & Shirato S, *Phys Lett B*, 391 (1997) 261.
22 Shyam R & Thompson I J, *Phys Rev C*, 59 (1999) 2645.
23 Margueron J, Bonaccorso A & Brink D M, *Nucl Phys A*, 703 (2002) 105.
24 Chatterjee R & Shyam R, *Phys Rev C*, 66 (2002) 061601.
25 Margueron J, Bonaccorso A & Brink D M, *Nucl Phys A*, 720 (2003) 337.
26 García-Camacho A, Nunes F M, Thompson I J, *Nucl Phys A*, 776 (2006) 118.
27 García-Camacho A, Nunes F M & Thompson I J, *Phys Rev C*, 76 (2007) 014607.
28 Kumar R & Bonaccorso A, *Phys Rev C*, 84 (2011) 014613.
29 Kumar R, Bonaccorso A, *Phys Rev C*, 86 (2012) 061601.
30 Surender & Kumar R, *Acta Phys Pol B*, 54 (2023).
31 Fu Y, Qin-Yuan Z, Zhi-Gang W & Xiang-Zhou C, *Phys Rev C*, 84 (2011) 037603.
32 Langer C, Scheit H, Boretzky K, Heine M, Johansson H, Oliveira J R B, Sumikama T, Suzuki D & Yosoi K, *Phys Rev C,* 89 (2014) 035806.
33 Bennett M B, Hitt G W, Bardayan D, Blackmon J C, Brune C R, Chae K Y, Champagne A E, Johnson M S, Kozub R L & Nesaraja C D, *Phys Rev C*, 97 (2018) 065803.
34 Xiang-Zhou C, Jun X, Zhi-Gang W & Qin-Yuan Z, *Chin Phys Lett*, 19 (2002) 1068.
35 Togano Y, Nakamura T, Kondo Y, Tostevin J A, Aoi N, Fukuda N, Gomi T, Ishihara M, Kobayashi T & Kubo T, *J Phys: Conf Ser*, 312 (2011) 042025.
36 Trache L, Azhari A, Clark H L, Fu C, Banu A, Tribble R E, 10th *Symp Nuclei Cosmos*, NIC 10, (2009).
37 Wrede C, Brown B A, Bardayan D W, Blackmon J C, Champagne A E, Daigle S, Hatarik R, Kolata J J, Lewis R & Roberts D A, *Phys Rev C*, 79 (2009) 045808.
38 Äystö J, Yli-Kojola K, Trzaska W H & Antony M S, *Phys Scr*, T5 (1983) 193.
39 Saastamoinen A, Beard M, Görres J, Trache L, Tribble R E, *AIP Conf Proc*, 1409 (2011) 71.
40 Äystö J, Yli-Kojola K, Trzaska W H & Antony M S, *Phys Lett B*, 110 (1982) 437.
41 Goriely S, Samyn M & Pearson J M, *Phys Rev C*, 75 (2007) 064312.
42 Audi G, Wapstra A H & Thibault C, *Nucl Phys A*, 729 (2003) 337.
43 Bertulani C A & Alexandra G, *Comput Phys Commun*, 175 (2006) 372.